Design of Dynamic Scaled Model of Wings Using Multi-Material Topology Optimization

Alessandro Brogliato[1,✉]

[1]Advanced composites Group, Instituto Superior Técnico, Av. Rovisco Pais 1, 1049-001 Lisbon, Portugal

The dynamic behavior of an aircraft can be investigated through computation or experiments. To validate their designs, engineers need to perform experiments that are usually expensive and time-consuming. In order to improve this process, topology optimization can be used to produce scaled models with the same dynamic behavior of the full-scale model that requires smaller testing facilities and less time to be produced thanks to the potentialities of additive manufacturing. The goal of this work is to produce a scaled model that has the same dynamic behavior as the full-scale model. The method used to obtain this result is the multi-material topology optimization where the material properties are defined using the Solid Isotropic Material with Penalization method. The Modal Assurance Criterion is selected as the optimization constraint to track and synthesize modes between the full scale and the scaled designs. Eigenvector derivatives must be calculated and two different methods were used in order to calculate the sensitivities.

Introduction

The optimization process adopted in this work aims to generate a scaled model of a wingbox that presents similar characteristics to a compared full scale wing-box. The objective function of the optimization will be the minimization of the difference of the eigenfrequencies of the models and the inequality constraints are based on the modal assurance criteria. This approach guides the optimization to obtain, as mentioned before, matching natural frequencies and eigenmodes.
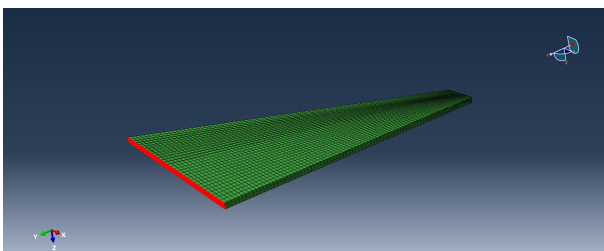

Fig. 1. Representation of the wing-box

In this extended abstract the case study in exam is going to be presented with the definition of the optimization problem, the computational environment and finally the results obtained.

Case Study

The case in exam uses a structure, called wing box, that is an idealization of a real wing-box present inside the skin of the wing in a normal aircraft. This element is designed to provide the necessary strength in the lightest way possible and usually it is composed by numerous ribs and spars. The wing-box used, being a simplification, is a sandwich structure. This type of structure is composed by two thin and strong skins divided by a thick layer of lightweight core that can be a foam or an honeycomb. The core main function is to separate the two skins and carry the load from one skin to the other and, while slightly increasing the weight, it dramatically increases the inertia of the whole structure improving bending and buckling loads (1).

The 3D model for the finite element analysis is presented in figure 1, the dimensions of the box are reported in table 1. The scaling factor between the two models is 10 and therefore the natural frequencies and the modal displacement will need to be scaled by a factor of 10 in order to be directly compared (2).

Instance	Full Scale Model [mm]	Scaled Model [mm]
Base Chord	3200	320
Tip Chord	500	50
Half Wingspan	4600	460
Thickness	100	10

Table 1. Model dimensions comparison

The mesh of the skin is composed by shell elements, and the mesh of the internal core is globally composed by 19200 hexahedral 3D elements divided in 8 layers of 2400 cells each. Only the internal core is included in the optimization process while the skin material distribution does not change during the optimization. The great computational time required to perform the optimization however requires to simplify the model and reduce the number of cells used, the patch approach is therefore used. The patch used in the optimization is applied at a layer level, every patch contains 12 cells and the material properties of the sub-cells are the same if they are shared by the same patch.

Optimization Problem

The optimization problem studied in this work is to minimize the function f:

$$f = \sum_{i=n}^{n}(1 - \frac{\omega_{scaled}(i)}{\omega_{full}(i)})^2 \qquad (1)$$

Subject to the constraint *g(i)*:

$$g(i) = 1 + \gamma - MAC(i,i) \quad with \quad \gamma = 10^{-6} \qquad (2)$$

where ω is the solution to the problem $(K - \omega^2 M) = 0$ and MAC is calculated with the formula presented in the paragraph at page 3 of this extended abstract.

Sequential Approximate Optimization

Sequential Approximate Optimization has been selected for the purpose of this study because the number of variables in the simulation is considerably high and other methods would result computationally expensive.

Considering the kth iteration with l the number of equality constraints, m the number of inequality constraints, n the number of design variables, $\bar{f}_0^k$ is the approximated function of f_0 and $\bar{g}_0^k$ $\bar{h}_0^k$ are the approximated functions of the equality and inequality constraints; the problem can be expressed as follows:

$$minimize \ \bar{f_0^k}(x)$$

$$\begin{cases} \bar{g}_0^k(x) = 0, \ j = 1,...,l \\ \bar{h}_0^k(x) \leq 0, \ j = 1,...,m \\ \alpha_i^k \leq x_i \leq \beta_i^k \ i = 1,...,n \end{cases} \qquad (3)$$

where x is the vector containing the design variables, k is the number of design variables and α and β are the limits for the optimization of the considered function at the considered iteration.

Computational Structure

The process of optimization requires to continuously analyze the structure in order to update the results. The process is controlled by Matlab that performs the optimization but in order to compute the structure fundamental frequencies and the related eigenmodes, the use of Abaqus is required.

Matlab communicates to Abaqus using Python scripts so the whole process is automatized and at every iterations the information is stored in *.txt* files in order to prevent data losses in case of unexpected crashes.

The computational process starts from a Matlab code that launches the finite element analysis of the full scaled model using a pre-compiled python code that contains all the information needed by the finite element code to run. After convergence of the simulation of the full scale model, the initial design is updated and the pre-processing is completed.

When the pre-processing is completed the optimization loop can start and it is composed by three separate main sequences:
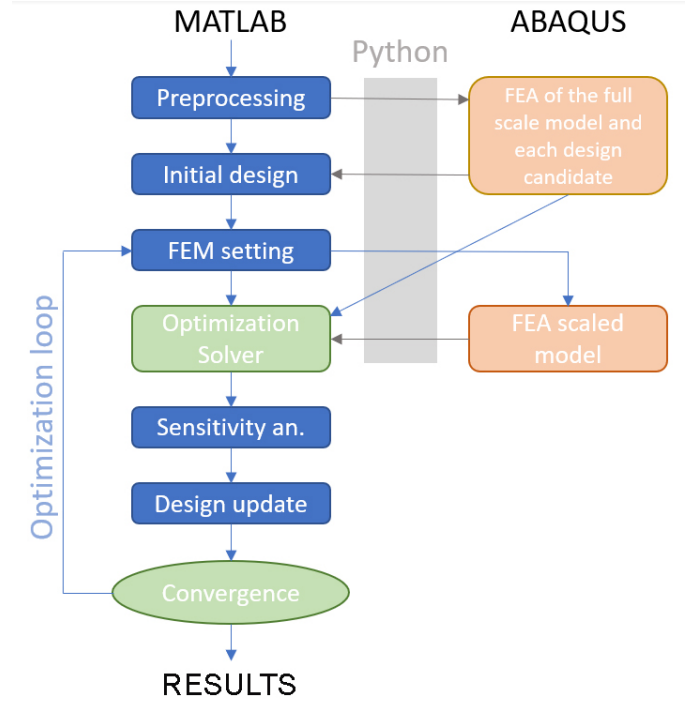

Fig. 2. Computational Structure

- Scaled model FEA

- Sensitivity analysis

- Optimization algorithm

The scaled model analysis is performed in the same way it is performed in the pre-processing, but differently from the full scale model analysis, it is performed every time the design is updated and therefore for every optimization loop. After the simulation has converged the results of the simulation is imported in the Matlab environment in the form of global variables in order to share them with the various functions of the code. The variables imported are essentially the eigenfrequences and eigenvectors of the structure and the stiffness matrices that are needed in order to perform the sensitivity analysis. Once the sensitivity analysis is completed the objective function, it's derivative, the inequality constraints and their derivatives are imported into IPOPT (3) and the code performs the optimization that leads to a new material distribution.

The optimization loop is then iterated until the maximum number of iterations is reached.

Solid Isotropic Material with penalization

Solid Isotropic Method with Penalization has been proposed by Bendsøe and Kikuchi (4) in 1989 and then by Rozvany and Zhou in 1991 (5). The method prevents the formation of grey areas in the optimized structure. Gray areas are particularly problematic because they represent a material that was not expected at the beginning of the optimization or simply does not exist. The stiffness is defined by the following formula:

$$E(\rho_e) = \rho_e^p E_0 \qquad (4)$$

E defines the Young Modulus of every element in the discretization and ρ is the density relative to the element. This definition indicates that if p=1, E/E_0 varies linearly between 0 and 1 while if $p > 1$, E/E_0 assumes an exponential behaviour prioritizing external values and therefore avoiding grey areas.

Modal Assurance Criterion

The Modal Assurance Criterion, is a statistical indicator sensible to the differences between mode shapes. In general it can be used in order to compare:

- Experimental eigen-vectors and analytical mode shapes.

- A defined mode shape with a modified one.

It is important in our case because it allows the code to directly compare the mode shapes of the full scaled wing-box and of the scaled wing-box; when comparing a set of mode shapes it returns an array of values between 0 and 1 where 1 means complete similarity and 0 means total difference but values over 0.9 already indicate a consistent correspondence and are acceptable for the purpose of the test (6).

$$MAC(r,q) = \frac{|\{\phi_A\}_r^T * \{\phi_X\}_q|^2}{(\{\phi_A\}_r^T * \{\phi_A\}_r) * (\{\phi_Q\}_q^T * \{\phi_Q\}_q)}$$

Where ϕ_A is the eigenvector related to the full scaled model and ϕ_X is the eigenvector related to the scaled model.

Adjoint method

The Adjoint Method, developed by Tsai ad Cheng (7), requires five steps in order to be performed, the eigenvectors of the two structures and the global matrices of the scaled model are required as an input. It is important to remark that the method cannot distinguish the eigenvectors in the case of repeated eigenvalues. The solution adopted by Tsai is to maximize the natural frequencies, which provides an easy and straightforward way to prevent mode switching, (7) which is not applicable in this case study and therefore extra attention needs to be used to monitor mode switching:

- $a = ((\frac{(\psi_0^T \psi_j)}{(\psi_0^T \psi_0)(\psi_j^T \psi_j)})\psi_0^T - (\frac{(\psi_0^T \psi_j)^2}{(\psi_0^T \psi_0)(\psi_j^T \psi_j)^2})\psi_j^T)\psi_0^T$

- $c = ((\frac{(\psi_0^T \psi_j)}{(\psi_0^T \psi_0)(\psi_j^T \psi_j)})\psi_0^T - (\frac{(\psi_0^T \psi_j)^2}{(\psi_0^T \psi_0)(\psi_j^T \psi_j)^2})\psi_j^T) - 2a\psi_0^T M$

- $\alpha_p = \frac{K - \lambda M}{c}$

- $b = -\alpha_p M \psi_0^T$

- $\alpha_j = b\psi_0^T + \alpha_p$

The MAC derivatives in the adjoint method are calculated using the global mass and stiffness matrices of the scaled model. Since the global matrices are not normally given as an output by Abaqus, a new instance of Abaqus has to opened ever iteration adding computational time. The steps used in the calculation are the following, α_j is then used by the equation to calculate the derivatives of the Modal Assurance Criterion:

$$\frac{\partial MAC}{\partial \rho} = \alpha_j \frac{\partial K}{\partial \rho}\psi_j + (a\psi_j - \lambda\alpha_j)\frac{\partial K}{\partial \rho}\psi_j$$

Multi-material topology optimization

The topology optimization includes three different materials, in this case the elastic modulus can be expressed by the equation:

$$E(\rho_1, \rho_2) = \rho_1^{pe}(\rho_2 E_1 + (1 - \rho_2^{pe})E_2)$$

Where we are neglecting the importance of the third material that is void and in the code is indicated with a value of 10^{-8} GPa instead of zero in order to avoid numerical instabilities. The element constitutive matrix C_e is expressed as the linear combination of the constitutive matrices of the materials:

$$C_e = \sum_{k=1}^{m} \omega_k C_k \quad with \quad \sum_{k=1}^{m} \omega_k = 1$$

Results

The case presented is the case that presented the best results in terms of material distribution and natural frequency matching. As presented in table 2 the materials used are two with a Young modulus of respectively 4 and 1 GPa. The penalization factor used is equal to 3 and a density filter is applied to the optimization.

| Penalization factor = 3			
Material	E [GPa]	$\rho[kg/m^3]$	ν
Core (Full Scale)	0.03	1000	0.32
Skin (Full Scale)	70	2700	0.33
Core 1 (Scaled)	4	1180	0.3
Core 2 (Scaled)	1	1150	0.3
Core 3 (Scaled)	$1e^{-8}$	10	0.3
Skin (Scaled)	70	2700	0.33

Table 2. Material properties of case 5

The optimization targeted the first three eigenfrequencies, and the results show a percentage deviation lower than 1% for all the targeted modes.

Mode	Scaled	Full scale	Full scale *10	% difference
1	34.89	3.52	35.19	0.86
2	111.08	11.16	111.55	0.43
3	137.67	13.87	138.66	0.72

Table 3. Natural frequency comparison

The objective function converged to zero fairly quickly while the convergence of the function related to the inequality constraints diverged until iteration 100 and then started to get smaller.
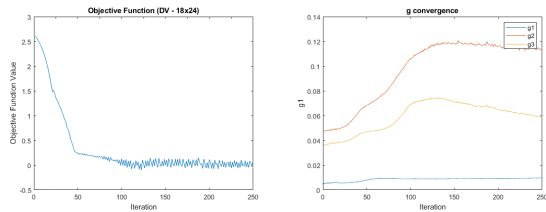

**Fig. 3.** Objective function and constraint function convergence.
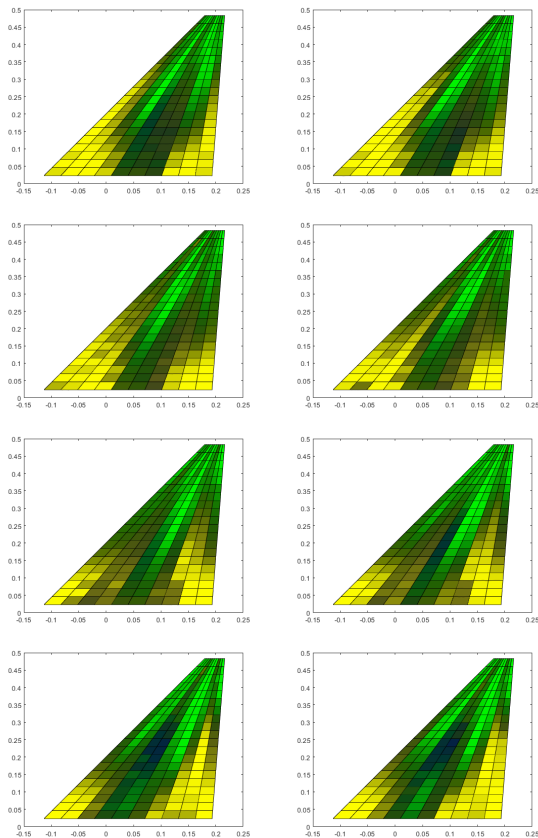
Fig. 4. Material distribution after the optimization ordered from layer 1 to layer 8.

The MAC related to the first three modes is higher than 0.95 for the first two modes that are represented by figure 5 and 6 while is lower than 0.9 for figure 7. This is visible in the figures where a bigger difference is displayed by 7. More iterations should be performed to evaluate the fitting of mode three.
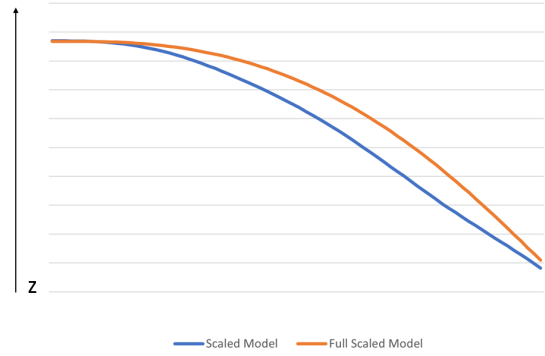
Fig. 5. Mode 1 mid-chord spanwise displacement (bending)
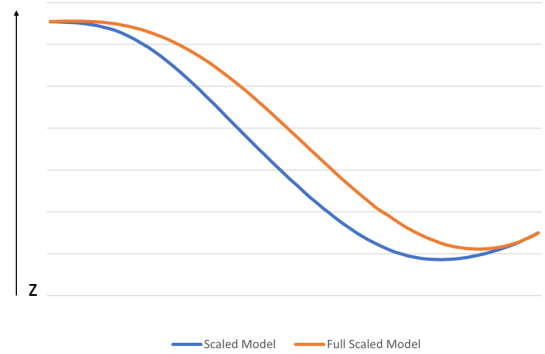
Fig. 6. Mode 2 mid-chord spanwise displacement (bending)
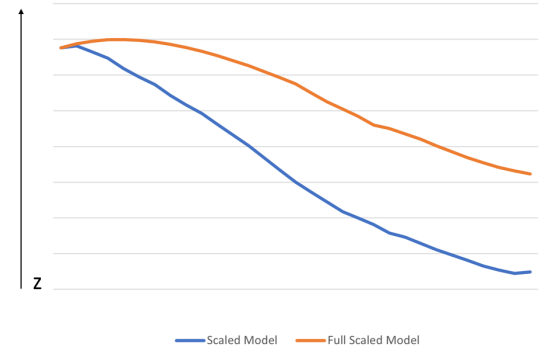
Fig. 7. Mode 3 chord displacement (torsion)

Conclusion

The results obtained, show that the code was able to produce designs with eigenfrequencies comparable to the one of the full scaled model with errors under 1%. The first and the second eigenmodes have been represented quite carefully by every simulation but the third mode, a torsional mode, has to be improved.

The results could be improved increasing the number of patches and therefore the computational time but this was not feasible with the setup used for the work in exam.

The drawback that the simulation displayed is that the influence of multiple materials have not made a considerable impact on the results since most of the final designs preferred the first material, the stiffest one, than the second. It is possible to see this in figure 4 where material number 2 is absent from the figure. This behaviour has to be investigated with the selection of different materials.

For the future developments of the work some aspects should be underlined:

- Ulterior simulations with an higher number of patches should be performed in order to obtain a better fit for the third vibrational mode.

- The application of different filtering techniques in order to obtain a smoother solution and allow the 3D printed manufacturing of a real model.

- The introduction of lattice cells in the optimization in order to allow intermediate designs in the 3D printing.

- To physically produce the final design and to test its dynamical properties in a wind tunnel in order to validate the model. This implementation is feasible for two main reasons, the size of the scaled model could potentially fit in a large number of wind tunnels and the materials used in the implementations are chosen with material properties that are close to the ones of polymers available for FDM printers.

Bibliography

1. D. Zenkert. *An Introduction to Sandwich Construction*. Engineering Materials Advisory Services, 1995. ISBN 9780947817770.
2. Anshuman Jha, Ramin Sedaghati, and Rama Bhat. Dynamic testing of structures using scale models. volume 9, 04 2005. ISBN 978-1-62410-065-9. doi: 10.2514/6.2005-2259.
3. A Wächter, Lorenz Biegler, Yi-dong Lang, and Arvind Raghunathan. Ipopt: An interior point algorithm for large-scale nonlinear optimization, 01 2002.
4. Martin Philip Bendsøe and Noboru Kikuchi. Generating optimal topologies in structural design using a homogenization method. *Computer Methods in Applied Mechanics and Engineering*, 71(2):197–224, 1988. ISSN 0045-7825. doi: https://doi.org/10.1016/0045-7825(88)90086-2.
5. M. Zhou and G.I.N. Rozvany. The coc algorithm, part ii: Topological, geometrical and generalized shape optimization. *Computer Methods in Applied Mechanics and Engineering*, 89(1):309–336, 1991. ISSN 0045-7825. doi: https://doi.org/10.1016/0045-7825(91)90046-9. Second World Congress on Computational Mechanics.
6. M. Pástor, Michal Binda, and Tomáš Harčarik. Modal assurance criterion. *Procedia Engineering*, 48:543–548, 12 2012. doi: 10.1016/j.proeng.2012.09.551.
7. T. D. Tsai and C. C. Cheng. Structural design for desired eigenfrequencies and mode shapes using topology optimization. *Struct. Multidiscip. Optim.*, 47(5):673–686, May 2013. ISSN 1615-147X. doi: 10.1007/s00158-012-0840-2.